Physical properties of $(PPO)_n(LiTFSI)$ polymer electrolytes: nuclear magnetic resonance investigation and comparison with $(PEO)_n(LiTFSI)$

1996 J. Phys.: Condens. Matter 8 7005

(http://iopscience.iop.org/0953-8984/8/38/005)

J. Phys.: Condens. Matter **8** (1996) 7005–7017. Printed in the UK

Physical properties of $(PPO)_n$(LiTFSI) polymer electrolytes: nuclear magnetic resonance investigation and comparison with $(PEO)_n$(LiTFSI)

C Roux†‡, W Gorecki‡, J-Y Sanchez†, M Jeannin‡ and E Belorizky‡

† Laboratoire d'Ionique et d'Electrochimie des Solids (Unité associée au CNRS 1213), Institut National Polytechnique de Grenoble, BP 75, 38402 Saint Martin d'Hère Cédex, France

‡ Laboratoire de Spectrométrie Physique (Unité associée au CNRS 08), Université J Fourier, BP 87, 38402 Saint Martin d'Hères Cédex, France

Received 8 February 1996, in final form 13 May 1996

Abstract. The physical properties of the ionic conductor $(PPO)_n(Li^+[(CF_3SO_2)_2N]^-)$, obtained by dissolution of lithium trifluoromethanesulphonylimide in poly(propylene oxide), have been investigated for several values of n. The glass transition temperature T_g has been established from both DSC and NMR techniques. The diffusion coefficients of ^{19}F-containing species have been determined by the pulsed magnetic field gradient technique. The behaviour of the proton relaxation time T_1 versus temperature and concentration has been correlated to the glass temperature. The behaviour of the proton transverse relaxation function, obtained by the spin-echo technique, has been interpreted using a simple model in which two regimes and consequently two transverse relaxation times coexist and are assigned to the 'entangled' and 'non-entangled' parts of the high-molecular-weight polymer chains investigated.

1. Introduction

Polymer electrolytes, i.e. ionic conductors resulting from the complexation of low-lattice-energy salts with solvating polymers, have generated over the past decade a widespread and sustained interest [1–3]. Such materials are expected to be used for applications in electrochemical devices, especially in lithium secondary batteries.

The most studied substrate is still poly(ethylene oxide) (PEO) which has extremely strong solvating properties for a wide variety of salts through interaction of the ether oxygen atoms with cations [4]. However, a serious limiting factor has been recognized for this host polymer, namely its semicrystalline character at room temperature. Indeed nuclear magnetic resonance (NMR) gave the first indication that the amorphous phase is responsible for ionic conductivity [5]. *A priori*, it is then interesting to investigate host polymers that overcome this drawback but keep the same cation solvating potentiality. For this purpose we investigated the poly(propylene oxide) (PPO) host polymer with the formula $-[CH_2CH(CH_3)O]_n-$. For several adjacent units, the relative positions of the methyl groups can be randomly distributed and this leads to an amorphous macromolecular structure.

Many investigations have been undertaken and, in particular, Chabagno [6] carried out an extended study of the ionic conductivities on various alkaline salts dissolved in PPO: $LiClO_4$, $LiCF_3SO_3$, LiSCN and $LiPh_4$. As expected, lithium PPO electrolytes are more conducting than the corresponding semicrystalline POE-based complexes, with the same salts, at ambient temperature. However, at high temperatures, as soon as its crystalline parts

0953-8984/96/387005+13$19.50

melt, PEO electrolytes become completely amorphous and provide larger ionic conductivities than the corresponding PPO complexes. This is probably due to the reduced solvating power and/or to the lower chain mobility of PPO polymer.

We have recently investigated the physical behaviour of $(PEO)_n$(LiTFSI) (where LiTFSI is lithium trifluoromethanesulphonylimide) [7] displaying the outstanding property of almost complete dissociation of the salt. It was therefore natural to make a comparison with the corresponding $(PPO)_n$(LiTFSI) complexes.

2. Experimental details

2.1. Samples

PPO is synthesized at 100 °C under argon at 7 bar in a Parr reactor vessel. All components were handled in a glove-box under anhydrous argon (less than 1 ppm H_2O and O_2). The polymerization process takes 24 h. More details about this coordinated polymerization have been given elsewhere [8]. The resulting polymer has a high $\bar{M}_w \approx 600.000$ g mol^{-1} and a polymolecularity index $I = \bar{M}_w/\bar{M}_n = 2.0$. As will be shown below, it behaves like a highly amorphous material.

PEO of molecular weight $\bar{M}_w \approx 900.000$ g mol^{-1} and $I \approx 2.2$ was supplied by Aldrich and LiTFSI by Hydro-Quebec.

The polymer complexes were prepared in a dry glove-box under argon, by dissolving in the polymer the pre-weighed amount of salt at the desired O to Li ratio in dry acetonitrile. After stirring, the homogeneous solution was outgassed under partial vacuum and cast onto a PTFE-lined plate. Then the electrolyte, kept dust free, was left at ambient temperature to evaporate the solvent without bubble formation. To complete the drying, the films were held at 40 °C under vacuum for several days.

For each salt concentration, only one membrane was used for all physical and electrochemical experiments. From this membrane, a disc and two small samples were extracted to perform conductivity, differential scanning calorimetry (DSC) and NMR analyses, respectively.

2.2. Differential scanning calorimetry

DSC traces were obtained under helium using a Netszch STA 409 instrument between 170 and 420 K. At least two heating sequences were applied to the samples in order to obtain reliable values of T_g.

2.3. Nuclear magnetic resonance

Five kinds of experiment were performed with NMR techniques.

(i) The free induction decay $G(t)$ was measured in order to check the salt concentration of the various samples. The magnitude of the signal, immediately after the $\pi/2$ pulse, $M_x(0) = \text{constant} \times G(0)$, is directly proportional to the number of resonating nuclei. Then, by comparing the signals of protons and ^{7}Li nuclei of our samples with several references involving the same nuclei with well established composition, it is possible to derive a rather accurate value of n. These comparisons must be performed under strictly the same experimental conditions.

(ii) The free induction decay was measured to determine the transition temperature T_g independently of the DSC data. By increasing the temperature in steps of 5 K from 160 K

at the rate of 0.2 K mn^{-1} to ensure thermal equilibrium at each step, the curves of $\log[g(t)]$ versus t, where $g(t)$ is the reduced relaxation function, display a very slight temperature dependence for $T < T_g$ and split into several branches for $T > T_g$. Consequently, the time t_1, for which $g(t_1) = 1/e$, remains almost constant at low temperatures and then sharply increases at a temperature corresponding to T_g. Note that this method provides an accurate determination of T_g and is equivalent to the classical technique performed from the observation of the drop of the second moment, the measurement of which was not possible in the equipment available to us.

(iii) The longitudinal relaxation times T_1 of the protons and of the ^{7}Li nuclei were measured with the usual inversion recovery sequence (π–τ–$\pi/2$). We used a superconducting magnet, allowing us to work at 245 MHz and 95 MHz for ^{1}H and ^{7}Li, respectively.

(iv) The transverse relaxation times T_2 of ^{1}H, ^{7}Li and ^{19}F nuclei were measured by the usual Hahn spin-echo technique with a ($\pi/2$–τ–π–τ) sequence, using the superconducting magnet for ^{1}H and ^{7}Li and a magnet allowing us to work at 80 MHz for ^{19}F.

(v) The diffusion coefficients D of the ^{19}F nuclei were measured through the pulsed magnetic field gradient technique (PMFG) using the sequence described by Stejskal and Tanner [9]. Let τ be the time interval between the initial $\pi/2$ pulse and the π pulse, which is equal to the time interval between the π pulse and the echo signal. Denoting by $A(2\tau)$ and $A^*(2\tau)$ the amplitudes of the echo in the absence and in the presence, respectively, of the gradient pulses one has, for a nucleus with a gyromagnetic factor γ,

$$\log[A^*(2\tau)/A(2\tau)] = -\gamma^2 D g^2 \delta^2 (\Delta - \delta/3)$$

where g is the magnitude of the two gradient pulses, Δ the time interval between these pulses and δ their duration. In our experiment, g was varied between 0 and 600 G cm^{-1}, Δ between 30×10^{-3} and 60×10^{-3} s, and δ was fixed at 8×10^{-3} s. This allowed us to observe the attenuation of a spin-echo amplitude over a range of about 30, providing good accuracy (5%) of the values determined for the self-diffusion constants.

3. Results and discussion

3.1. Structural information

The DSC traces of five different pure PPO samples were investigated in order to check the small degree of crystallinity of this polymer. In the first heating sequence, at a rate of 20 K min^{-1}, only one sample displayed very small endothermic peaks at around 313 K. This can be explained by very slow recrystallization kinetics, which was strongly dependent on the storage temperature and varied for each sample. Consequently it can be considered that pure PPO is almost purely amorphous.

The DSC traces of $(PPO)_n$(LiTFSI) for $n = 5$, 7, 18 are shown in figure 1. Only the second heating sequence, at a rate of 20 K min^{-1} is displayed, as no change was observed in the following heating sequence. Note that the first heating sequence gave erratic data, probably owing to poor thermal contact between the polymer sample and the vessel. From these curves, it is easy to determine the transition temperature T_g between the vitreous and the amorphous states from the jump of the specific heat C_p, which is proportional to dH/dt. It can be seen that T_g increases regularly with increasing salt concentration up to $n = 5$ from $T_g = 207$ K to $T_g = 273$ K. This behaviour is very similar to those observed for PEO and PPO complexes [10]. The salt concentration of each sample was checked using the NMR technique described in (i) in section 2.3, with four different reference samples of

$(PEO)_n$(LiTFSI). The T_g-values have been determined through the method described in (ii) of section 2.3. In figure 2, we plot for $(PPO)_n$(LiTFSI) the temperature dependence of the time t_1 defined above. Typically, for $n = 5$, t_1 remains almost constant and then sharply increases at a temperature $T = 265$ K, compared with the value $T_g = 273$ K obtained by DSC. The slight difference between these temperatures is due not only to the uncertainty of the experimental procedure but also to the large difference between the heating rates in both methods.

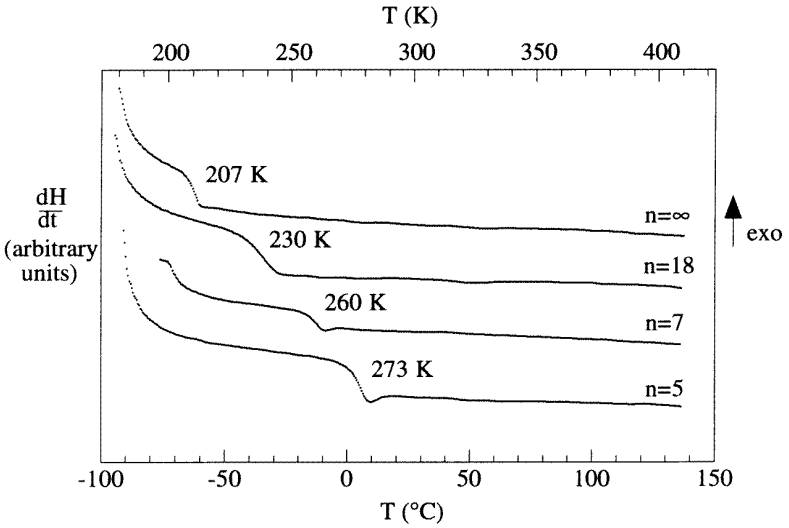

Figure 1. DSC traces for $(PPO)_n$(LiTFSI) in second heating sequence at a rate of 20 K min^{-1}.

In table 1 we compare the various T_g-values obtained from DSC and NMR techniques. The general agreement is quite satisfactory.

Table 1. Vitreous transition temperatures T_g of $(PPO)_n$(LiTFSI) for different values of n, obtained through DSC and NMR measurements.

	T_g (K)	
n	DSC	NMR
∞ (pure PPO)	207	200
18	230	225
7	260	245
5	273	265

3.2. Relaxation processes

A study of the longitudinal relaxation times versus temperature of the protons was performed for several salt concentrations in the amorphous state. The results are shown in figure 3. In the range 290 K $< T <$ 380 K, for pure PPO, T_1 increases with increasing temperature. However, for salt complexes, with increasing concentration the inverse phenomenon occurs; T_1 decreases more and more rapidly when T increases.

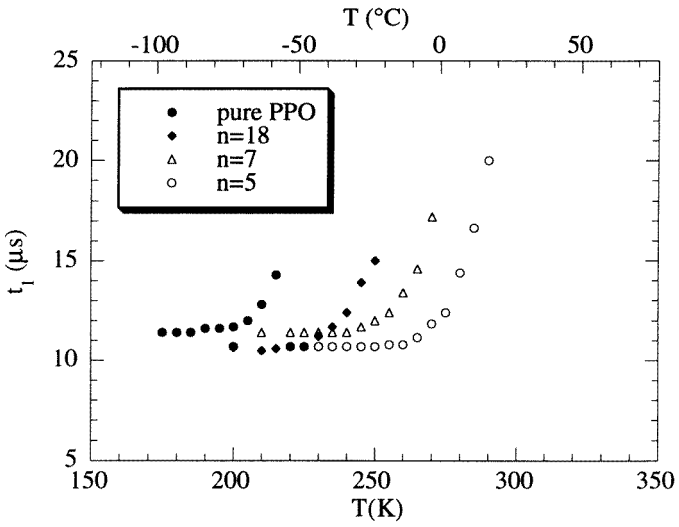

Figure 2. Characteristic times t_1 (see text) at various temperatures for different salt concentrations of $(PPO)_n$(LiTFSI).

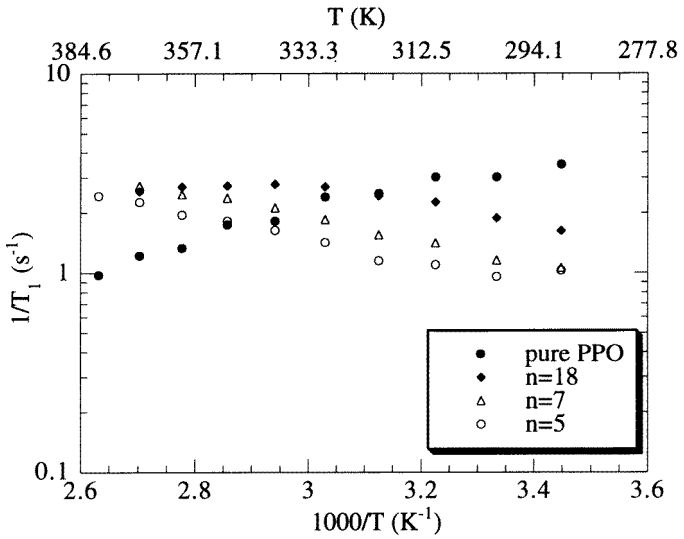

Figure 3. Proton longitudinal relaxation rates $1/T_1$ of $(PPO)_n$(LiTFSI) versus temperature (resonance frequency $\nu_1 = 245$ MHz).

This behaviour may be understood by considering a relaxation process of the protons dominated by magnetic dipole–dipole interactions with other protons [11] and following the Vogel–Tamman–Fulcher (VTF) model [12] for the correlation time τ_c, which is given by

$$\tau_c = \tau_0 \exp\left(\frac{B}{k_B(T - T_0)}\right) \tag{1}$$

where B is a pseudo-activation energy and T_0 is the ideal glass transition temperature.

$T_g - T_0$ is typically 40–50 K [13]. In our case, T_0 is taken to be $T_g - 50$ K in PEO complexes, and $T_g - 45$ K in $(PPO)_8(LiTFSI)$.

If $\omega_I \tau_c \ll 1$, $1/T_1$ is proportional to τ_c and $\log(1/T_1)$ decreases when T is higher as observed for pure PPO. If $\omega_I \tau_c \gg 1$, $1/T_1$ behaves like τ_c^{-1} and $\log(1/T_1)$ increases with increasing temperature, as observed for salt polymer complexes. Furthermore, for a given value of T, when the salt complex is more concentrated, T_0 increases and $1/T_1$ decreases, in agreement with the results displayed in figure 3.

Contrary to what is observed for $(PEO)_8(LiClO_4)$ [14], the maximum of the curve of $\log(1/T_1)$ versus $1000/T$ corresponding to $\omega_I \tau_c \approx 1$ is not observed for $(PPO)_n(LiTFSI)$ in the temperature range investigated except for $n = 18$. In this case the maximum occurs at $T = 345$ K. This means that the theoretical maximum occurs at higher temperatures for $(PPO)_n(LiTFSI)$ than for the corresponding PEO complexes. This phenomenon is directly related to the difference in the T_g-values of both series ($T_g(PEO) < T_g(PPO)$), leading for a given temperature to a higher τ_c-value for $(PPO)_n(LiTFSI)$ than for the corresponding PEO complexes. Our results suggest that the PPO-based complexes have lower mobility than the PEO complexes, in agreement with the results observed for PPO and PEO–$LiClO_4$ complexes [15].

We represent in figure 4 the behaviour of $\log(1/T_1)$ versus $1000/(T - T_0)$ with $T_0 = T_g - 45$ K for different salt concentrations using the glass transition temperatures given in table 1. The various curves almost coalesce, giving satisfactory agreement with the VTF model. This means that above T_g the relaxation process is related to the strong narrowing of the observed NMR line due to the onset of polymer chain motion.

Simultaneously, we performed measurements of the longitudinal relaxation times versus temperature of the ^{7}Li nuclei for several salt concentrations. As for the proton relaxation rates, the maximum of $1/T_1$ is not observed except for $n = 18$. For all the other polymer salt concentrations, T_1 decreases both with increasing salt concentrations and with increasing temperature. The overall behaviour of the ^{7}Li relaxation is very similar to that observed for the protons. However, contrary to what is observed for $(PEO)_n(LiTFSI)$ complexes [7] it is not possible to unify the various curves within the VTF model. It can be argued that there is a correlation between the dynamics of the cations and the PPO chains but that additional physical processes are involved. It is expected [16] that in PPO complexes the cations are less easily solvated than in PEO complexes. A non-negligible fraction of the cations may then associate and not follow the chain dynamics.

An extensive study of the proton transverse relaxation rates $1/T_2$ of high-molecular-weight $(PPO)_n(LiTFSI)$, with the usual spin-echo technique at 245 MHz, was undertaken.

We display in figure 5 the time variation in the echo signal amplitude $g(t = 2\tau)$ for $(PPO)_8(LiTFSI)$ at various temperatures. Similar sets of curves were obtained for different values of n. Note that the value $G(0)$ is extrapolated from the free induction decay signal immediately after the $\pi/2$ pulse.

In figure 6 we show the time variation in the echo signal amplitude $g(2\tau)$ at two fixed temperatures $T = 310$ K and $T = 370$ K for various salt concentration of $(PPO)_n(LiTFSI)$.

The most striking feature displayed by figure 6 is that for any concentration and any temperature the attenuation of $g(t)$ cannot be represented by a single-exponential function $g(t) = g(0)\exp(-t/T_2)$. For those high-molecular-weight polymers, we adapt the model of Cohen-Addad and Dupeyre [17] and Brereton [18] who extended ideas originally proposed by De Gennes [19] and Doi and Edwards [20] for 'entangled' polymer motion. The dynamics are characterized by two sets of chain relaxation times by introducing the submolecule concept currently used to describe viscoelastic properties. These two sets are well separated from each other. The longest relaxation times are associated with long-range

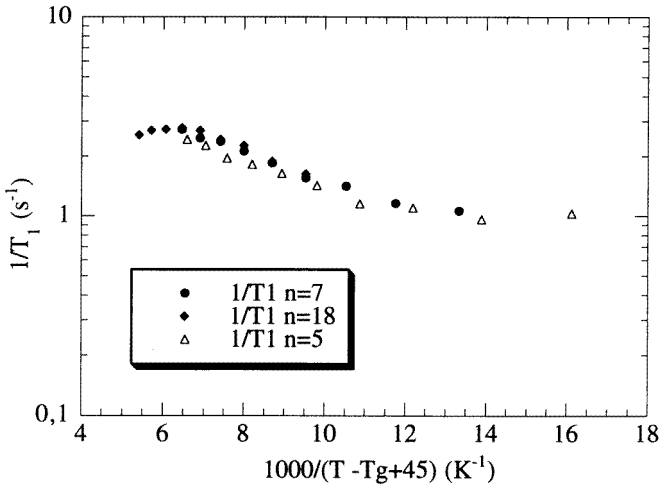

Figure 4. Proton longitudinal relaxation rates $1/T_1$ of $(PPO)_n$(LiTFSI) versus $1000/(T - T_0)$ with $T_0 = T_g - 45$ K (resonance frequency $\nu_I = 245$ MHz).

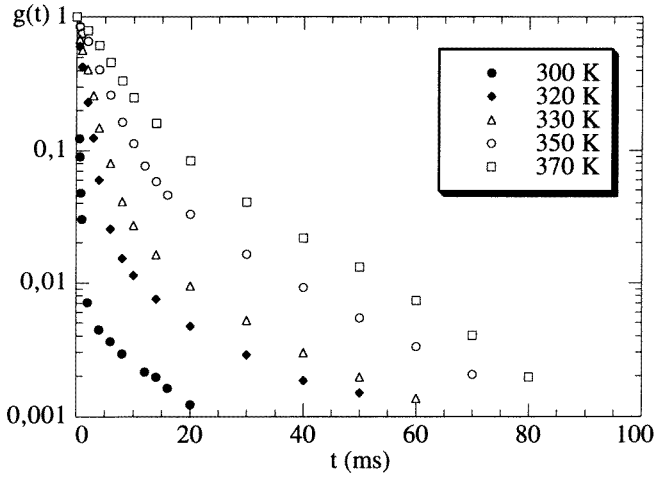

Figure 5. Normalized ^{1}H transverse relaxation of $(PPO)_8$(LiTFSI) obtained from the amplitude of the echo signal, for various temperatures with $T > T_g$ (resonance frequency $\nu_1 = 245$ MHz).

configurational changes involving disentanglement processes which are characterized by a correlation time τ_e. The short relaxation times are associated with short segment motions within submolecules, i.e. within the 'entangled' parts of the chain, and are characterized by a time correlation τ_R.

Here, in an operational way, we consider that we have proportions q and $1-q$ of 'non-entangled' and 'entangled' submolecules with correlation times τ_e and τ_R respectively. It is expected that $\tau_e < \tau_R$ as 'non-entangled' submolecules have slower relaxation rates. Then the relaxation function is given by

$$g(t) = q \exp(-t/T_2') + (1-q) \exp(-t/T_2) \tag{2}$$

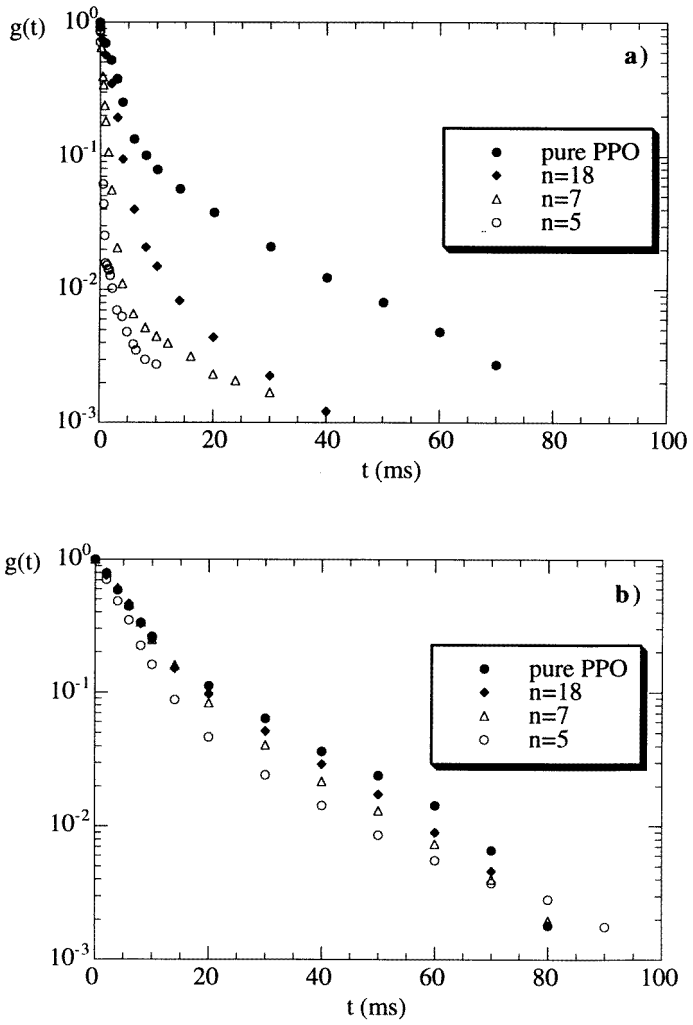

Figure 6. Normalized ^{1}H transverse relaxation function of $(PPO)_n$(LiTFSI) obtained from the amplitude of the echo signal, for various values of n at (a) $T = 310$ K and (b) $T = 370$ K (resonance frequency $\nu_1 = 245$ MHz).

with $g(0) = 1$.

Strictly speaking it would be more correct to write [21]

$$g(t) = q \exp(-t/T_2') + (1 - q)g_1(t)$$

where $g_1(t)$ corresponds to the 'entangled' part of the polymer and is characterized by a distribution of correlation times, leading to a stretched-exponential decay $g_1(t) = A \exp(-(t/T_2)^\alpha)$. As seen below, our data could be reasonably interpreted with equation (2) which will be used in this first approach. We represent in figure 7 the least-squares fits of the ^{1}H relaxation function $g(t)$ of $(PPO)_8$(LiTFSI), using the empirical equation (2). We have, for $T = 350$ K, $q = 0.07$, $T_2 = 4 \times 10^{-3}$ s and $T_2' = 19.4 \times 10^{-3}$ s. Note the remarkable agreement between the theoretical curve and the experimental results. The same procedure

was systematically performed for all our samples with various concentrations and at different temperatures above T_g. The results concerning the q values are summarized in table 2.

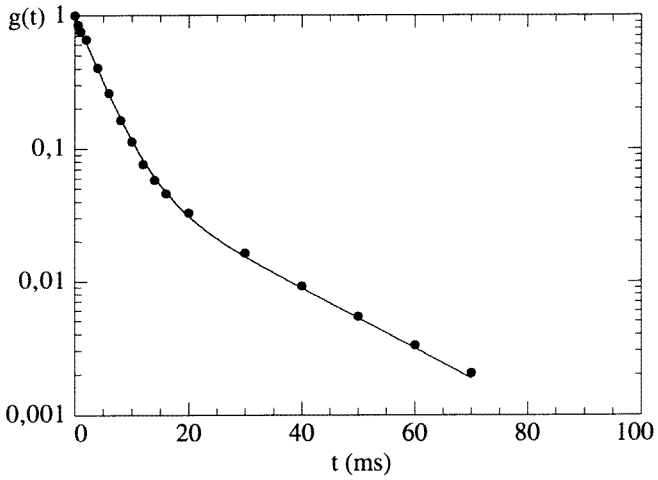

Figure 7. Fit of the ^{1}H normalized relaxation function of $(PPO)_8$(LiTFSI) to equation (2) (see text) for $T = 350$ K.

Table 2. Proportions q and $1-q$ of 'non-entangled' and 'entangled' polymer chains, respectively, for $(PPO)_n$(LiTFSI) with $n = \infty$, 18, 7, 5 for various temperatures.

	q; $1-q$			
T (K)	$n = \infty$	$n = 18$	$n = 7$	$n = 5$
300	0.07; 0.93	0.017; 0.983	0.005; 0.995	< 0.001; ≈ 1
330	0.13; 0.87	0.08 ; 0.92	0.022; 0.978	0.016; 0.984
350	0.2 ; 0.8	0.16 ; 0.84	0.07 ; 0.93	0.025; 0.975
370	0.28; 0.72	0.27 ; 0.73	0.25 ; 0.75	0.08 ; 0.92

It is observed that q is strongly correlated with the salt concentration for all temperatures. For pure PPO the values of q are 7% at 300 K and 28% at 370 K. For highly concentrated complexes ($n = 5$) these values are only from 0% and 8% at the same temperatures, respectively. This means that the salt favours the structural entanglement process. This result, characteristic of these high-weight polymers, is different from what is observed for lower-weight polymers ($\bar{M}_w = 20.000$ g mol^{-1}) of $(PEO)_n(LiCF_3SO_3)$ where q remains constant with n, showing that the ions do not introduce any topological constraint [22]. Furthermore, from the above table, it is seen that, as expected, q regularly increases with increasing temperature because thermal agitation leads to chain disentanglement.

The same temperature behaviour was observed for pure high-molecular-weight ($\bar{M}_w \approx$ 900.000 g mol^{-1}) PEO for $T > T_m$, where T_m is the melting temperature of the crystalline phase. However, for pure PEO the corresponding q-values are about a seventh of those of pure PPO. It seems therefore that entanglements are also related to the stereoregularity in adjacent units of the polymer chain. Pure PEO is more 'entangled' than pure PPO: $1 - q = 97.5\%$ and 80%, respectively, at 350 K.

Now we turn our attention to the transverse relaxation times T_2 and T_2' obtained by our fitting procedure. The results are shown in figure 8 for several salt concentrations and various temperatures. The corresponding ratios T_2'/T_2 are listed in table 3 for $n = \infty$ and 18.

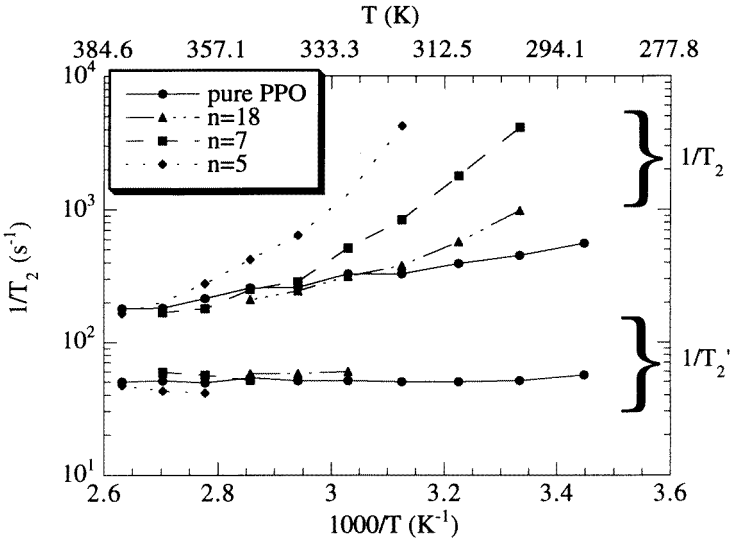

Figure 8. Proton transverse relaxation times T_2 and T_2' versus temperature of $(PPO)_n$(LiTFSI) for various values of n (resonance frequency $\nu_1 = 245$ MHz). T_2 and T_2' refer to the 'entangled' and 'non-entangled' parts, respectively, of the polymer (see equation (2)). When the q-values are lower than 5%, the uncertainty in T_2' is very large and the corresponding values are not shown.

Table 3. Ratios T_2'/T_2 for protons in $(PPO)_n$(LiTFSI) for various temperatures.

	T_2'/T_2	
T (K)	$n = \infty$	$n = 18$
330	6.4	5.2
350	4.8	3.6
370	3.5	3

We have $3 \leqslant T_2'/T_2 \leqslant 6$, and in the Brereton model this would correspond to a ratio τ_R/τ_e between the same limits. It should be pointed out that, for $(PEO)_n(LiCF_3SO_3)$ chains of molecular weight 20.000, τ_R/τ_e was nearly constant and close to 3.5. From figure 8 we see that in the high-temperature region the ratio T_2'/T_2 becomes almost independent of salt concentration with $T_2'/T_2 \approx 3.5$. The ^{1}H transverse relaxation times are governed by proton–proton and proton–lithium magnetic dipole interactions. As the limiting relaxation behaviour at high temperatures of the various salt complexes is identical with that of pure PPO, this means that the dipolar interaction with the ^{7}Li nuclei becomes negligible and consequently that the motion of the Li^+ ions is little affected at high temperatures by the entanglement process. In other words the characteristic time t corresponding to the presence

of the Li ion in the solvation sphere of the polymer chain becomes extremely short.

The same analysis for pure PEO gives a ratio T_2'/T_2 of the order of 10 at 370 K. Furthermore T_2 is about half that in pure PPO. This is in agreement with our previous result on the respective values of q for both compounds, showing that PEO is more 'entangled' than PPO. This remark is consistent with the fact that PEO has a higher density (1.3) than PPO (1.01) [23] despite the larger monomer weight of the latter. However, in PPO, one should not forget the fact that, owing to the fast rotation of the methyl groups, both the intramolecular and intermolecular dipolar interactions contribute less to the relaxation rate than in PEO. This effect partly explains the larger values of T_2 in PPO than in PEO.

3.3. Diffusion coefficients

We measured the diffusion coefficients of the (TFSI) anion, through the NMR signal of the ^{19}F ($I = 1/2$) nuclei by the PMFG technique described in section 2. We denote by ^{19}D these diffusion coefficients which were determined for different salt concentrations of $(PPO)_n$(LiTFSI) at various temperatures. The results are shown in figure 9. As expected, ^{19}D increases with increasing temperature. The curves of $\log(^{19}D)$ against $1000/T$ are almost linear within the experimental error and we can extract the activation energies $^{19}E_A$ which are listed in table 4.

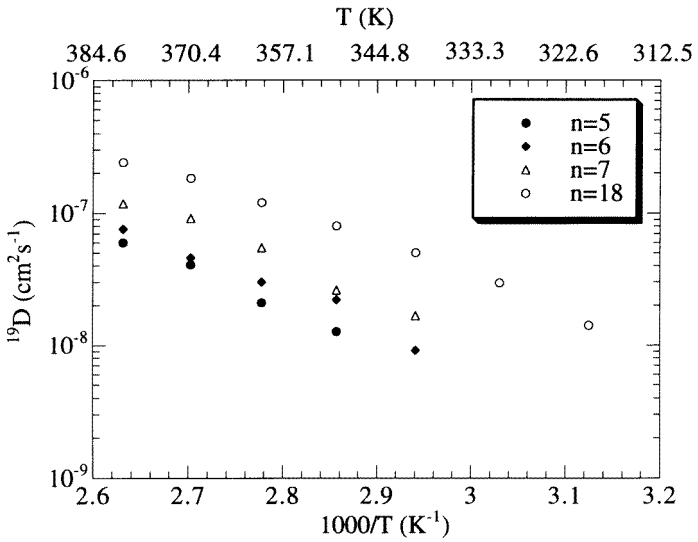

Figure 9. Temperature dependence of the ^{19}D diffusion constants of $(PPO)_n$(LiTFSI) (resonance frequency $\nu_1 = 80$ MHz).

The apparent activation energies $^{19}E_A$ are almost independent of n. Furthermore the absolute values of ^{19}D decrease with increasing salt concentration, in agreement with the higher proportion of 'entangled' chains and of the sample viscosity.

Finally we compare the above results with those corresponding to $(PEO)_n$(LiTFSI) [7]. The apparent fluorine activation energies $^{19}E_A$ of salt PPO complexes are about 20% higher than in PEO complexes. In table 5 we list the absolute values of ^{19}D for both series of compounds at a fixed temperature $T = 370$ K.

Generally the fluorine diffusion coefficients in PPO salt complexes are about a half or

Table 4. Apparent activation energies $^{19}E_A$ characteristic of the anionic diffusion coefficients obtained from figure 9.

n	$^{19}E_A$ (eV)
18	0.52
7	0.5
5	0.43

Table 5. Diffusion coefficients ^{19}D of $(PPO)_n$(LiTFSI) and $(PEO)_n$(LiTFSI) at $T = 370$ K.

	$^{19}D \times 10^8$ (cm^2 s^{-1})	
n	$(PPO)_n$(LiTFSI)	$(PEO)_n$(LiTFSI)
20		60
18	20	
10		30
8		25
7	9.1	
6	4.6	10
5	4	

a third of those in PEO salt complexes, in agreement with our prediction resulting from analysis of the T_1 relaxation results (section 3.1). This proves that the mobility of the chains is higher in POE complexes than in PPO complexes at a fixed salt concentration and temperature. For PEO polymers it is well established [24] that the ionic transport numbers t^- are three to five times larger than the cationic transport numbers t^+. Furthermore the ratio of the conductivity of the amorphous PEO complex to that of the amorphous PPO complex [25] varies from 2 at 370 K to 12 at 294 K. Then, if it is assumed that the ratio t^-/t^+ is of the same order in both families, the relative values of the diffusion coefficients are consistent with the conductivity measurements.

4. Conclusion

The T_g-values for pure PEO ($T_g = 213$ K) and pure PPO ($T_g = 207$ K) are very close as well as for dilute electrolyte polymers but T_g increases more rapidly in concentrated PPO complexes than in the corresponding PEO complexes.

The longitudinal relaxation times T_1 of the protons in $(PPO)_n$(LiTFSI) can be well described using the VTF model with an ideal glass transition temperature $T_0 = T_g - 45$ K. We have shown that in this series the protons have a lower mobility than in $(PEO)_n$(LiTFSI). Our results concerning the transverse relaxation times of the proton can be interpreted by a simple model involving two distinct dynamical behaviours corresponding to the 'entangled' and 'non-entangled' parts of the polymer chain and leading to two well separated relaxation times. This model provides the respective proportions of the submolecules belonging to the different regimes and shows that the salt favours the structural 'entanglement' process in PPO complexes. Furthermore, in the framework of our simple model, pure PEO appears more 'entangled' than pure PPO at a given temperature. Our results are consistent with the observation of a shorter T_2 in PEO than in PPO although this effect is partly due to the fast

rotation of the methyl group. On the other hand, the fact that T_2' is about 50% larger in pure PEO than in pure PPO is not yet explained but is probably related to the higher observed mobility of PEO chains.

Finally, the diffusion coefficients ^{19}D of the fluorine anions in $(PPO)_n$(LiTFSI) were shown to be about half the corresponding diffusion constants for $(PEO)_n$(LiTFSI) complexes, a result which is consistent with conductivity measurements in both series.

Several complementary data are still to be measured such as the diffusion constants of ^{1}H and ^{7}Li nuclei, in order to determine the ionic transport numbers. Furthermore a detailed analysis of the relaxation mechanisms of ^{7}Li and ^{19}F nuclei is required to obtain more information about the solvation process of the salt molecules with the polymer chains.

Acknowledgments

This work was partially supported by Hydro-Québec through the ACEP project. We express our gratitude to Dr E Geissler for fruitful comments.

References

[1] MacCallum J R and Vincent C A (ed) 1987–9 *Polymer Electrolytes Review*—1,2 (London: Elsevier)
Bruce P G and Vincent C A 1993 *Faraday Trans.* **89** 3187
[2] Gray F M 1991 *Solid Polymer Electrolytes* (Weinheim: VCH)
[3] Skotheim T A (ed) 1988 *Electroresponsive Molecular and Polymeric Systems* vol 1 (New York: Marcel Dekker)
Takeoka S, Ohno H and Tsushida E 1993 *Polym. Adv. Technol.* **4** 53
[4] Armand M 1990 *Adv. Mater.* **2** 6
[5] Berthier C, Gorecki W, Minier M, Armand M Chabagno J-M and Rigaud P 1983 *Solid State Ion.* **11** 91
[6] Chabagno J-M 1980 *Doctoral Thesis* University of Grenoble
[7] Gorecki W, Jeannin M, Belorizky E, Roux C and Armand M 1995 *J. Phys.: Condens. Matter* **7** 6823
[8] Roux C and Sanchez J-Y 1994 *Solid State Ion.* **72** 160
[9] Stejskal E O and Tanner J E 1965 *J. Phys. Chem.* **42** 288
[10] Armand M, Gorecki W and Andréani R 1990 *Proc. 2nd Int. Symp. on PE* (London: Elsevier) p 91
[11] Abragam A 1961 *The Principles of Nuclear Magnetism* (Oxford: Oxford University Press)
[12] Vogel H 1921 *Phys. Z.* **22** 645
Tamman G and Hesse W 1926 *Z. Anorg. (Allg.) Chem.* **156** 245
Fulcher G S 1925 *J. Am. Ceram. Soc.* **8** 339
[13] Brown S D, Greenbaum S G, McLin M G, Wintersgill M C and Fontanella J J 1994 *Solid State Ion.* **67** 257–62
[14] Donoso J P, Bonangamba T J, Panepucci H C, Oliveira L N, Gorecki W, Berthier C and Armand M 1993 *J. Chem. Phys.* **98** 10 026
[15] Donoso J P, Bonagamba T J, Frare P L, Mello N C, Magon C J and Panepucci H 1995 *Electrochim. Acta* **40** 2361
[16] Armand M, Chabagno J M and Duclot M 1979 *Fast Ion Transport in Solids* ed P Vashita, J N Mundy and G K Shenoy (Amsterdam: North-Holland) p 131
[17] Cohen-Addad J P and Dupeyre R 1983 *Polymer* **24** 400
[18] Brereton M G 1990 *Macromolecules* **23** 1119
[19] de Gennes P G 1979 *Scaling Concepts in Polymer Physics* (Ithaca, NY: Cornell University Press)
[20] Doi M and Edwards S F 1986 *The Theory of Polymer Dynamics* (Oxford: Clarendon) ch 7.3
[21] Kimmich R, Kopf M and Callaghan P 1991 *J. Polym. Sci.* B **29** 1025
[22] Ries M E, Brereton M G, Cruickshank J M, Klein P G and Ward I M 1995 *Macromolecules* **28** 3282
[23] Booth C, Devoy C J, Dogson D V and Hiller I H 1970 *J. Polym. Sci.* A **8** 519
[24] Armand M 1994 *Solid State Ion.* **69** 309
[25] Roux C and Sanchez J-Y 1995 *Electrochim. Acta* **40** 8953